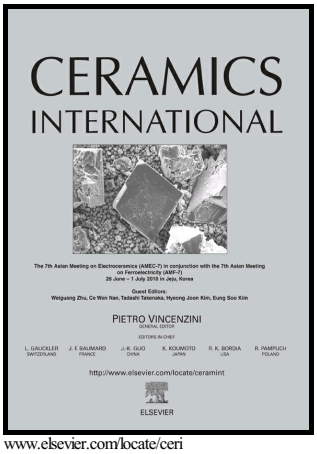

www.elsevier.com/locate/ceri

Influence of the microstructure on the thermal shock behavior of cemented carbides

Jose Maria Tarragó, Selassie Dorvlo, Joan Esteve, Luis Llanes

PII: S0272-8842(16)30614-9
DOI: http://dx.doi.org/10.1016/j.ceramint.2016.05.024
Reference: CERI12826

To appear in: *Ceramics International*

Received date: 14 April 2016
Revised date: 29 April 2016
Accepted date: 5 May 2016

Cite this article as: Jose Maria Tarragó, Selassie Dorvlo, Joan Esteve and Lui Llanes, Influence of the microstructure on the thermal shock behavior o cemented carbides, *Ceramics Internationa* http://dx.doi.org/10.1016/j.ceramint.2016.05.024

Influence of the microstructure on the thermal shock behavior of cemented carbides

Jose Maria Tarragó[a,b,1], Selassie Dorvlo[c], Joan Esteve[d], Luis Llanes[a,b,*]

[a]CIEFMA, Departament de Ciència dels Materials i Enginyeria Metal·lúrgica, Universitat Politècnica de Catalunya, ETSEIB, Barcelona, 08028, Spain

[b]CRnE, Centre de Recerca en Nanoenginyeria, Universitat Politècnica de Catalunya, Barcelona, 08028, Spain

[c] Sandvik Hyperion, Coventry, CV4 0XG, UK

[d] Departament de Física Aplicada i Óptica, Universitat de Barcelona, Barcelona, 08028, Spain

[*]luis.miguel.llanes@upc.edu

ABSTRACT

The influence of single and repetitive sudden changes of temperature on the mechanical integrity of cemented carbides was investigated as a function of their microstructure. Thermal shock resistance was assessed by testing the residual flexural strength of hardmetal beams after being subjected to thermal shock by water quenching. Results indicate that hard cemented carbides tend to exhibit a superior resistance to the nucleation of thermal shock damage but a lower resistance to the propagation of thermal shock than tough cemented carbides, and vice versa. These trends are in agreement with those expected from the evaluation of the thermal shock Hasselman's parameters. The evidenced strength loss after thermal shock may be related to the subcritical growth of intrinsic

[1] Current address: Sandvik Mining and Construction Tools AB. Västberga, Stockholm 0120, Sweden.

flaws based on localized microcracking. Results also point out on Ni-based hardmetals to exhibit a slightly higher resistance to abrupt changes of temperature than Co-based ones.

KEYWORDS

Cemented carbides; Thermal shock; Hasselman parameters; Fractography; Strength degradation

1. INTRODUCTION

Cemented carbides, usually referred to as hardmetals, are composite materials consisting of hard ceramic particles embedded in a tough metallic matrix acting as a binder. They exhibit an exceptional combination of strength, toughness and wear resistance as a result of the extremely different properties of their two constitutive phases [1]. These merits endow hardmetals as first choice materials for a wide range of severe applications, including exposure to harsh service conditions such as corrosive environments, high temperatures or abrupt temperature changes [2]. Nevertheless, despite its exceptional thermal conductivity and excellent fracture toughness in comparison with ceramic materials, WC-Co cemented carbides are sensitive to thermal shock due to its brittle-like nature behavior [3,4]. Thus, thermal cracking and thermal fatigue are recognized as common modes of failure of cemented carbide tools in different applications, such as in intermittent cutting and rock drilling [5–9]. However, different from the case where pure mechanical loads are implied [9,10], studies devoted to thermal shock resistance of hardmetals are relatively scarce [3,4,11–15]. Further, these studies only relate to Co-base hardmetals and the influence of the microstructure on the strength degradation of these materials due to thermal shock is hardly addressed. Therefore, in this paper the influence of three different microstructural variables on the thermal shock resistance of cemented carbides are evaluated and discussed. These include: binder chemical nature, binder content, and carbide mean grain size. Within this context, it is worthy to remark that the replacement of Co metal by alternative binders is one of the major challenges of

hardmetals community [16]. That is particularly important nowadays, due to the classification of cobalt dust as a toxic and carcinogenic material by both, the European program for Registration, Evaluation, Authorisation and Restriction of Chemical substances (REACH) and the U.S. National Toxicology Program (NTP).

The measurement of the retained strength after a quench test is a common method for evaluating thermal shock resistance of ceramics. The test consists in determining the critical thermal shock temperature difference (ΔT_c) above which the residual strength is reduced up to values of 70% the average strength measured at room temperature [17]. Aiming to rationalize thermal shock rupture, Hasselman theory is frequently invoked to describe the strength degradation of ceramic materials when the microstructure has a critical role in defining thermal shock resistance. It consists of several thermal shock resistance parameters (i.e. *R* parameters) that define the resistance of the material to crack initiation and/or propagation due to sudden temperature changes. Indeed, first Hasselman thermal shock parameter (i.e. the *R* parameter) was firstly defined by Kingery [18]. A few years later, Hasselman proposed the *R''''* parameter [19] and the unified theory of thermal shock [20]. In this investigation, both Hasselman's parameters, *R* and *R''''*, are recalled for the analysis of the microstructural effects on the thermal shock behavior of hardmetals. The *R* parameter refers to the critical quenching temperature to induce fracture in the material and can be estimated according to:

$$R = \frac{\sigma_r(1-\nu)}{E\alpha} \qquad (1)$$

where σ_r is the fracture strength, ν is the Poisson ratio, E is the elastic modulus and α is the coefficient of thermal expansion. On the other hand, the *R''''* parameter describes the condition necessary for the propagation of thermal shock induced cracks and is given by:

$$R'''' = \frac{1}{2(1-\nu)}\left(\frac{K_{Ic}}{\sigma_r}\right)^2 \qquad (2)$$

where K_{Ic} is the fracture toughness of the material. Within this framework, Mai [3] documented a strong strength degradation of cemented carbides when subjected to abrupt temperature changes, and successfully rationalized strength loss with crack initiation (R) and crack propagation (R'''') Hasselman's thermal shock resistance parameters [20].

In addition to material properties and the critical temperature difference, there are several factors that have a relevant influence on the performance of a body subjected to thermal shock. Buessemen proposed a classification of these factors in three groups defining different issues [21]: (1) thermal shock conditions, (2) geometry of the solid body and (3) material properties. The first group includes temperature differential and heat transfer coefficient. The second one considers size and shape of the body. Finally, the third group accounts for coefficient of thermal expansion, elastic properties, fracture strength and fracture toughness [18,21]. The shape of the body is an extremely important aspect in determining the critical temperature difference. In general, it is recommended to avoid corners and edges, since they can act as thermal stress concentrators [18,21]. Hence, the critical temperature difference to crack a specimen can be defined as the crack initiation resistance parameter, multiplied by a shape factor (S) (i.e. $\Delta T_c = R \cdot S$) [18].

From a physical viewpoint, thermal shock damage in cemented carbides has been postulated to proceed mainly through the nucleation of microcracks at the carbide-binder interface which tend to propagate avoiding the hard phase [12–15]. This is due to the large difference between the coefficient of thermal expansion of the ceramic and metallic phases and because of the high elastic modulus of the composite material. Thus, abrupt temperature changes generate significant large thermal stresses that induce the formation of microcracks at the interface between carbide and binder [12,13]. Maximum cooling tensile stresses are concentrated at the surface, and the magnitude

of these induced stresses is a linear function of the temperature difference and the distance from the cooled surface [14,22]. In addition, the heat transfer coefficient between the coolant and the material has also a significant influence in the generation of thermal stresses. Within this context, water is found to be much more severe than silicon oil, and maximum thermal stresses are attained, when cooling hardmetals in water, at around 0.5 seconds after the first contact [14].

Similar to other metal-ceramic composite materials, cemented carbides exhibit a rising crack growth resistance (R-curve) behavior [23–26] related to the development of ductile bridging ligaments at the crack wake [25–27]. R-curve characteristics are strongly influenced by the microstructure, and R-curves with a more relevant increase (including a longer subcritical crack extension) are found when rising binder content and carbide mean grain size (i.e. higher fracture toughness). This crack bridging toughening mechanism translates into effective damage tolerance, becoming then a microstructural design strategy for improving the reliability of cemented carbides tools, wear parts and structural components.

In this paper, microstructural effects on the strength degradation of cemented carbides subjected to single and repetitive sudden temperature changes are studied. In doing so, and following the approach proposed by Mai [3], experimental data is analyzed and discussed on the basis of Hasselman's parameters for the assessment of thermal shock resistance in structural materials.

2. MATERIALS AND EXPERIMENTAL ASPECTS

2.1. Materials and microstructural characterization

Five experimental cemented carbides grades with different combinations of binder chemical nature (Co, CoNi and Ni) binder content (medium and high), and carbide mean grain size (ultrafine, fine, medium and coarse) were selected. All samples and materials used in this investigation were supplied by Sandvik Hyperion. Microstructural characteristics of studied hardmetals are given in

Table 1, and they include information on the binder chemical nature, binder weight content (V^{wt}_{binder}), carbide mean grain size (d_{WC}), carbide contiguity (C_{WC}) and binder mean free path (λ_{binder}). Within this context it is important to remark that the principal parameters used to characterize the microstructure of hardmetals are the binder volume and the carbide mean grain size. However, usually these two parameters are varied simultaneously, and consequently additional two-phase normalizing parameters are required in order to properly analyze microstructure-property correlations. Among them, the contiguity of the carbide phase, C_{WC}, and the binder mean free path, λ_{Co}, are the mostly employed ones. The former parameter describes the interface area fraction of carbides particles that is shared between them, whereas the latter refers to the mean size of the metallic phase. Binder content values are given as supplied by the manufacturer, whereas carbide mean grain size was measured following the linear intercept method in field emission scanning electron microscopy (FESEM) micrographs [28]. On the other hand, two-phase microstructural parameters, C_{WC} and λ_{binder}, were estimated from best-fit empirical equations given in the literature [29,30]. Further, it is important to remark that the investigated 10CoUF, 11CoM and 9NiF grades contain a small amount of Cr_3C_2, added as a grain growth inhibitor.

One main objective of this investigation is to correlate the strength loss induced by thermal shock in cemented carbides on the basis of the Hasselman parameters. The determination of the thermal shock resistance parameters requires of several material properties to be measured or estimated, the latter from equations proposed in literature. Measured and estimated properties at room temperature, together with the determined R and R'''' parameters for the studied materials are given in **Table 2**. The Poisson's ratio and the coefficient of thermal expansion were estimated by applying the rule of mixtures for composite materials. In doing so, the α and υ data for the WC and Co phases were collected from the investigation published by Mari *et al.* [31], whereas for the Ni binder a coefficient of thermal expansion similar to that of cobalt was chosen [32]. Hardness (*HV*) was measured using a Vickers diamond pyramidal indenter and applying a load of 294 N. Flexural

strength (σ_r) was assessed on four-point bending by means of a fully articulated test jig with inner and outer spans of 20 and 40 mm, respectively. These tests were performed on an Instron 8511 servohydraulic machine at a load rate of 100N/s. At least 15 specimens with dimensions of 45 mm x 3 mm x 4 mm (i.e. length x thickness x width) were tested per grade. The surface which was later subjected to the maximum tensile loads was polished to mirror-like finish and the edges were chamfered to reduce their effect as stress raisers. The same sample preparation and strength testing procedure was followed for the assessment of mechanical integrity of specimens subjected to sudden temperature changes. Fracture toughness (K_{Ic}) was determined by testing single edge pre-cracked specimens with dimensions of 45 mm x 5 mm x 10 mm at stress-intensity factor load rates of about 2 MPa√m/s, following the procedure described by Torres *et al.* [33]. Five samples were tested per studied hardmetal grade. Finally, the elastic modulus was assessed in the 45 mm x 3 mm x 4 mm bars by means of the "Impulse Excitation of Vibration" (IEV) method, according to the ASTM E-1876 standard [34].

2.2. Thermal shock tests

Thermal shock testing was performed by heating up the 45 mm x 3 mm x 4 mm bars at the desired temperature, and subsequently water quenching them. In doing so, the samples were heated at 10ºC/min in a Hobersal 12 PR/300 furnace to the intended temperature, held at the maximum temperature for 20 minutes to equilibrate it, and water quenched to room temperature (i.e. 23ºC). Two temperature differentials (ΔT) of 400ºC and 550ºC were selected. However, higher temperature difference levels were not tested, aiming to avoid interference of other environmental-related degradation phenomenon, i.e. oxidation [35,36]. Moreover, in order to assess the effect of repeated thermal shock, several samples were subjected to three different numbers of quenching cycles (N_c = 1, 3 and 10). Retained flexural strength at room temperature was measured by testing to failure at least 3 specimens per temperature difference and number of thermal shock repeats, following the

same procedure as the one done for the non-quenched (reference) bars. After failure, a detailed FESEM (JEOL-7001F unit) fractographic inspection was carried out in order to discern critical flaws that promoted rupture. The elastic modulus was also assessed after thermal shock tests (IEV method), in order to discern possible changes related to potential microcracking of the specimens. With that purpose at least three bars were tested per thermal shock condition and investigated material.

3. RESULTS AND DISCUSSION

Retained strength after water quenching against the number of thermal shock cycles is given in **Figure 1** for the two suddenly-induced temperature differentials investigated. **Figures 1a** and **1b** show the residual strength for temperature differentials of 400ºC and 550ºC, respectively. Experimental data is also plotted in **Figures 1c** and **1d**, but here the strength is normalized by using the fracture resistance measured in non-quenched specimens (reference baseline). These graphs clearly indicate that cemented carbides are sensitive to thermal shock. However, for the studied temperature differentials, and contrary to the case of other ceramics with lower toughness levels (e.g. [37,38]), an abrupt strength drop after thermal shock is not evidenced. Indeed, retained strength rather shows a slightly decrease when increasing temperature difference. Accordingly, strength retention after thermal shock at the tested temperature differences resulted to be always higher than 70% of the average room temperature strength, defined as the strength loss required for reaching ΔT_c. Those facts indicate that the critical temperature differential for studied materials is above 550 ºC. However, as previously commented, the samples were not heated up over this temperature differential to minimize oxidation damage [35,36]. Furthermore, relevant damage in the post-quenched study was also discerned as a function of the number of thermal shock cycles. In general, it can be observed that the retained strength decreases when increasing the number of cycles. This fact is more evident for the larger temperature differential. At this point it should be

mentioned that cemented carbides applications may imply higher thermal shock temperature differentials and larger number of thermal shock cycles [2,9]. Consideration of wider ranges of experimental variables was beyond the scope of this investigation, as main aim here was to provide a first insight into microstructural effects on the susceptibility of cemented carbides to be degraded due to thermal shock. Nevertheless, it is clear that further research involving higher temperature differentials and number of cycles, should be conducted if assessment of a damage scenario closer to real service-like conditions is wanted. The slight steady decrease of the retained strength observed when increasing the temperature differential and the number of quenching cycles, points out stable crack propagation of inherent cracks as the main thermal shock damage mechanism for strength degradation of cemented carbides [13]. In order to discern possible microcracking of the specimens, the elastic modulus was assessed after thermal shock and compared to that determined for the non-quenched specimens. However, no changes were evidenced in the stiffness of specimens after thermal shock, suggesting that microcracking was rather a localized phenomenon.

Experimental results indicate that for the studied ΔT of 400ºC almost no strength loss is evidenced in the first thermal shock cycle. For this sudden temperature change, retained strength after several thermal shock cycles is really close to that measured for non-quenched specimens. In fact, the observed strength loss was less than a 10% after the 10^{th} cycle for most of the studied hardmetals. The unique exception was the hardest (and most brittle) material, which exhibited a slightly higher strength loss (about 15%). The lowest damage tolerance to cyclic thermal shock crack propagation evidenced for the 10CoUF hardmetal is in agreement with the lowest estimated R'''' value for this grade. On the other hand, for the temperature differential of 550ºC, a significant strength drop at the 1^{st} thermal shock cycle was not evidenced for the harder and more brittle hardmetals (i.e. the 10CoUF and 9NiF grades). Meanwhile, the tougher grades exhibited strength drops between 10 and 15%. However, this trend was reversed when increasing the number of quenching cycles. Here, the largest strength loss after the repetitive 10^{th} thermal shock was found for the 10CoUF grade, while

the toughest material exhibited the best strength retention. These results are in complete agreement with the trends indicated by Hasselman's parameters, on the basis of strength retention after single or repetitive thermal shocks. Thus, the materials with higher *R* thermal shock parameter values exhibited better thermal shock resistance against damage nucleation (i.e. for the 1st quenching cycle), but were more sensitive to the propagation of this damage, as indicated by their lower *R''''* Hasselman parameter values.

The decision of which Hasselman parameter, *R* or *R''''*, is more adequate for the proper material selection against thermal shock mainly depends on the application. Within this context, Lu and Fleck [39] proposed two material performance indices for strength-controlled ($\sigma_r/E\alpha$) and toughness-controlled ($K_{Ic}/E\alpha$) failure. Both parameters consider a perfect heat transfer, but in the case of a poor surface heat transfer the heat conductivity (λ) must be also considered and included in both indices [39]. The first criterion considers tensile fracture in a solid containing a certain distribution of flaws, while the second assumes a large pre-existing flaw that fractures when the stress intensity factor at the crack tip reaches the fracture toughness value. Therefore, as it is the case for Hasselman parameters, the first is more related to crack initiation and the second to crack propagation [39]. An interesting tool for material selection against thermal shock is to represent in a map both merit indices, where $\sigma_r/E\alpha$ and $K_{Ic}/E\alpha$ are the horizontal and vertical axis, respectively. This map is shown for the studied cemented carbides in **Figure 2**. As evidenced from the Hasselman parameters, cemented carbides exhibiting a high strength-controlled merit index have small toughness-controlled indices, and vice versa. In this sense, the ideal material for thermal shock resistance would be the one combining high values for both parameters. It is interesting to note that the $(K_{Ic}/\sigma_r)^2$ parameter, which is proportional to the *R''''* thermal shock parameter, may be represented as parallel lines of constant $(K_{Ic}/\sigma_r)^2$ values in the map of **Figure 2**. Hence, materials with large $(K_{Ic}/\sigma_r)^2$ values exhibit a higher resistance to damage propagation, and therefore the $(K_{Ic}/\sigma_r)^2$ index can be interpreted as a measure of damage tolerance [39].

On the basis of the data shown in **Figure 2**, the 11CoM hardmetal grade exhibits the best compromise between both merit indices, and therefore it would be expected to have the best thermal shock resistance. However, this trend is not reflected on the retained strength values evidenced for this grade and shown in **Figure 1**. In this regard, it is interesting to highlight the relative high values of merit index for toughness-controlled fracture of medium and coarse-grained 10CoNiM and 10CoC grades, respectively. These values are in agreement with the high strength retention values evidenced for such grades (see **Figure 1**). Two main facts may explain this improved behaviour. First, damage tolerance levels increase when raising fracture toughness (i.e. when increasing the binder content and/or carbide mean grain size). Second, thermal conductivity of cemented carbides increases when raising the mean grain size of the carbide phase [40,41]. Therefore thermal gradients are reduced for coarser grades resulting in an enhanced resistance against sudden temperature changes. It will explain the improved thermal shock resistance evidenced for the coarser cemented carbides. On the other hand, and as already pointed out in previous investigations [42–44], it should be underlined the slightly improved strength retention observed for the studied nickel grades in comparison with Co-base hardmetals. Indeed, Co-binder phase in cemented carbides consists on a Co-W-C alloy due to the diffusion of W and C from WC into Co during the sintering process [45]. In this regard, the presence of both elements partially stabilizes the high temperature fcc phase [46,47], which is more ductile than the hcp room temperature phase. However, a phase transformation from the fcc phase to the hcp one is produced when subjecting the specimens to water quenching from temperatures around 600ºC [46]. Moreover, nickel binder accumulates deformation in the form of slip plus twinning damage mechanisms [48,49], but without evidence of such transformation. Therefore, the slightly higher strength losses evidenced for the Co-base grades could be speculated to be related to the fcc to hcp martensitic transformation induced during the thermal shock tests, that would not be taken place for nickel based cemented carbides.

Strength reduction due to thermal shock may be speculated to be associated with the inducement of thermal residual stresses (TRS) in the surface and/or with subcritical crack growth of pre-existing defects. In order to discern if abrupt temperature changes were promoting TRS that were interacting with applied loads, some 10CoUF samples were heat treated (after thermal shock tests) aiming to relieve them. Hence, the referred samples were heated up to 920ºC in a vacuum furnace, held for 1h at the maximum temperature and cooled again to room temperature [50,51]. These samples were then tested following the same procedure previously described for the assessment of flexural strength. Three different thermal shock conditions were evaluated and the obtained strength results after the heat treatment were compared to that exhibited by the quenched specimens (**Table 3**). The good agreement found between flexural strength results obtained for both conditions discards TRS as main reason for thermal shock degradation.

Finally, a detailed fractographic inspection of the broken specimens was conducted in order to identify the flaws that acted as initiation sites for failure as well as to discern additional damage induced by thermal shock. Some examples of the identified critical flaws are shown in **Figure 3**. Critical flaws origins mainly consisted on abnormally coarse WC particles (e.g. **Figure 3a** and **3c**) and binderless concentration of abnormally coarse WC particles (e.g. **Figures 3b**, **3d**, **3e** and **3f**); although other defect types such as inclusions and pores were identified for the hardest grades. In addition, the critical flaw sizes were estimated by means of linear elastic fracture mechanics (LEFM) and are shown in **Table 4**. This failure criterion relates the fracture strength with the critical flaw size (a_c) and the plane strain fracture toughness of the material according to the expression [52]:

$$K_{Ic} = Y\sigma_r\sqrt{a_c} \qquad (3)$$

where Y is a dimensionless crack/specimen geometric factor. In this investigation a Y value of 1.292 is considered, corresponding to semicircular surface cracks [53]. Experimentally determined and

estimated crack sizes are similar for the hard grades. However, this is not the case for the tougher ones, where LEFM analysis yield overestimated values. As previously reported by the authors of this investigation, these relative differences are related to the existence of an R-curve behavior in cemented carbides that becomes more prominent when rising fracture toughness. Details of this fracture mechanism may be found elsewhere [25]. According to LEFM estimates, critical flaws for the 10CoUF exhibit a subcritical crack grow from 10% up to 100% their original size, when subjected to 1 and 10 thermal shock cycles at a temperature differential of 550ºC, respectively. On the other hand, critical flaws for the tougher grade (i.e. 10CoC) are estimated to grow from 20% to 50% under the same thermal shock conditions. These results strengthen the arguments previously exposed: harder cemented carbides exhibit higher resistance to nucleation of thermal shock induced-damage, as compared to tougher grades, but lower to propagation of such damage.

In general, it was found that thermal shock cycles do not imply changes in the nature of failure controlling flaws in comparison with the identified flaws for non-treated specimens. Therefore, as previously commented, the nucleation of microcracks at the carbide-binder interfaces [12–15] in the vicinity of these critical defects may be postulated as the determining factor for strength loss associated with thermal shock. Under these conditions, microcracking is expected to promote subcritical growth of preexisting defects (and thus, may result in variations of their size and geometry). Consequently, a subsequent strength reduction of the material is to be expected. In this regard, several microcracks were evidenced in the regions close to the inherent critical defects at WC-binder interfaces, and are marked with arrows in **Figure 3**. This fact, in addition to the absence of variation in the elastic modulus after thermal shock tests, may explain the evidenced strength losses due to sudden temperature changes.

4. CONCLUSIONS

The resistance of cemented carbides to thermal shock was investigated by measuring the retained strength after subjecting the samples to single and repetitive abrupt temperature changes. In doing so, the thermal shock resistance of five hardmetals grades having different microstructural characteristics was assessed. Two temperature differences (400 and 550ºC) and three different numbers of thermal shock repeats (1, 3 and 10 quenching cycles) were selected for the thermal shock tests. Experimental results indicate that cemented carbides are sensitive to abrupt temperature changes and may experience important strength losses when subjected to thermal shock. Within the range of experimental variables investigated, the main change induced by thermal shock is speculated to be subcritical growth of the intrinsic flaws, as related to localized microcracking. Thus, as the number of thermal shock repeats increases, the effective size of potential critical defects becomes larger and corresponding flexural strength is increasingly lessened. The harder studied hardmetal grades exhibited a higher resistance to initiation of thermal shock-induced damage than the tougher ones. On the contrary, the harder grades were found to be more sensitive to the propagation of this damage. Such microstructural trends are in satisfactory agreement with those expected from the relative difference between their initiation (R) and propagation (R'''') Hasselman's parameters. The investigated Ni-based hardmetal exhibited a slightly superior thermal shock resistance than that expected for a WC-Co cemented carbide with alike microstructural characteristics. The higher strength losses evidenced for WC-Co hardmetals are postulated to be related to the martensitic phase transformation from the fcc to the hcp phase induced in the cobalt phase during quenching. An improved thermal shock resistance when increasing the mean carbide grain size was also evidenced, as related to a higher damage tolerance (i.e. due to a more prominent R-curve behavior) as well as to a higher thermal conductivity.

ACKNOWLEDGEMENTS

The authors would like to acknowledge I. Serra and W. Chen for their collaboration in the thermal shock testing as well as in the discussion of the results. This work was financially supported by the Spanish Ministerio de Economía y Competitividad (Grant MAT2012-34602 and MAT2015-70780). Additionally, J.M. Tarragó acknowledges the Ph.D. scholarship received from the collaborative Industry-University program between Sandvik Hyperion and Universitat Politècnica de Catalunya.

References

[1] H.E. Exner, Physical and chemical nature of cemented carbides, Int. Met. Rev. 24 (1979) 149–173.

[2] L. Prakash, Fundamentals and general applications of hardmetals, in: V.K. Sarin, D. Mari, L. Llanes (Eds.), Comprenhensive Hard Materials, Elsevier, UK, 2014: pp. 29–90.

[3] Y.W. Mai, Thermal-shock resistance and fracture-strength behavior of two tool carbides, J. Am. Ceram. Soc. 59 (1976) 1–4.

[4] C.W. Merten, Response of a WC–Co alloy to thermal shock, in: R.K. Viswanadham, D.J. Rowcliffe, J. Gurland (Eds.), Proceedings of the 1st International Conference on the Science of Hard Materials, Plenum Press, New York, 1983: pp. 757–774.

[5] M. Lagerquist, A study of the thermal fatigue crack propagation in WC–Co cemented carbide, Powder Metall. 18 (1975) 75–87.

[6] H. Chandrasekaran, Fracture of carbide tools in intermittent cutting, in: R.K. Viswanadham, D.J. Rowcliffe, J. Gurland (Eds.), Proceedings of the 1st International Conference on the Science of Hard Materials, Plenum Press, New York, 1983: pp. 735–755.

[7] J. A. Ghani, C.H. Che Haron, S.H. Hamdan, A.Y. Md Said, S.H. Tomadi, Failure mode analysis of carbide cutting tools used for machining titanium alloy, Ceram. Int. 39 (2013) 4449–4456.

[8] J. Xiong, Z. Guo, M. Yang, W. Wan, G. Dong, Tool life and wear of WC–TiC–Co ultrafine

cemented carbide during dry cutting of AISI H13 steel, Ceram. Int. 39 (2013) 337–346.

[9] L. Llanes, M. Anglada, Y. Torres, Fatigue of cemented carbides, in: V.K. Sarin, D. Mari, L. Llanes (Eds.), Comprenhensive Hard Materials, Elsevier, UK, 2014: pp. 345–362.

[10] A.V. Shatov, S.S. Ponomarev, S.A. Firstov, Fracture and strength of hardmetals at room temperature, in: V.K. Sarin, D. Mari, L. Llanes (Eds.), Comprenhensive Hard Materials, Elsevier, UK, 2014: pp. 301–343.

[11] D. Hand, J.J. Mecholsky, Strength and toughness degradation of a tungsten carbide-cobalt due to thermal shock, J. Am. Ceram. Soc. 73 (1990) 3692–3695.

[12] S. Ishihara, T. Goshima, K. Miyao, T. Yoshimoto, S. Takehana, Study on the thermal shock behavior of cermets and cemented carbides, Japan Soc. Mech. Eng. Solid Mech. Mater. Eng. 34 (1991) 490–495.

[13] S. Ishihara, T. Goshima, K. Nomura, T. Yoshimoto, Crack propagation behavior of cermets and cemented carbides under repeated thermal shocks by the improved quench test, J. Mater. Sci. 34 (1999) 629–636.

[14] T. Yoshimoto, S. Ishihara, T. Goshima, A.J. McEvily, T. Ishizaki, An improved method for the determination of the maximum thermal stress induced during a quench test, Scr. Mater. 41 (1999) 553–559.

[15] S. Ishihara, H. Shibata, T. Goshima, A.J. McEvily, Thermal shock induced microcracking of cermets and cemented carbides, Scr. Mater. 52 (2005) 559–563.

[16] S. Norgren, J. García, A. Blomqvist, L. Yin, Trends in the P/M hard metal industry, Int. J. Refract. Met. Hard Mater. 48 (2015) 31–45.

[17] ASTM C1525 - 04: Standard test method for determination of thermal shock resistance for advanced ceramics by water quenching, USA, 2014.

[18] W.D. Kingery, Factors affecting thermal stress resistance, J. Am. Ceram. Soc. 38 (1955) 3–15.

[19] D.P. Hasselman, Elastic energy at fracture and surface energy as design criteria for thermal shock, J. Am. Ceram. Soc. 46 (1963) 535–540.

[20] D.P. Hasselman, Unified theory of thermal shock fracture initiation and crack propagation in

brittle ceramics, J. Am. Ceram. Soc. 52 (1969) 600–604.

[21] W.R. Buessem, Thermal shock testing, J. Am. Ceram. Soc. 38 (1955) 15–17.

[22] Z.-H. Jin, Y.-W. Mai, Effects of damage on thermal shock strength behavior of ceramics, J. Am. Ceram. Soc. 78 (1995) 1873–1881.

[23] P.A. Mataga, Deformation of crack-bridging ductile reinforcements in toughened brittle materials, Acta Metall. 37 (1989) 3349–3359.

[24] Y. Torres, D. Casellas, M. Anglada, L. Llanes, Fracture behavior of hardmetals: implementation of flaw configuration modeling and R-Curve concepts, in: H. Danninger, R. Ratzi (Eds.), Proceedings Euro PM 2004, EPMA, Vienna, Austria, 2004: pp. 551–556.

[25] J.M. Tarragó, E. Jiménez-Piqué, L. Schneider, D. Casellas, Y. Torres, L. Llanes, FIB/FESEM experimental and analytical assessment of R-curve behavior of WC-Co cemented carbides, Mater. Sci. Eng. A. 645 (2015) 142–149.

[26] J.M. Tarragó, D. Coureaux, Y. Torres, D. Casellas, I. Al-Dawery, L. Schneider, L. Llanes, Microstructural effects on the R-curve behavior of WC-Co cemented carbides, Mater. Des. 97 (2016) 492–501.

[27] L.S. Sigl, H.E. Exner, Experimental study of the mechanics of fracture in WC–Co alloys, Metall. Trans. A. 18A (1987) 1299–1308.

[28] ISO 4499-2 Hardmetals. Metallographic determination of microstructure. Part 2: Measurement of WC grain size, Switzerland, 2008.

[29] J. Gurland, New scientific approaches to development of tool materials, Int. Mater. Rev. 33 (1988) 151–166.

[30] J.M. Tarragó, D. Coureaux, Y. Torres, F. Wu, I. Al-Dawery, L. Llanes, Implementation of an effective time-saving two-stage methodology for microstructural characterization of cemented carbides, Int. J. Refract. Met. Hard Mater. 55 (2016) 80–86.

[31] D. Mari, B. Clausen, M. Bourke, K. Buss, Measurement of residual thermal stress in WC–Co by neutron diffraction, Int. J. Refract. Met. Hard Mater. 27 (2009) 282–287.

[32] A.D. Krawitz, E.F. Drake, B. Clausen, The role of residual stress in the tension and compression response of WC–Ni, Mater. Sci. Eng. A. 527 (2010) 3595–3601.

[33] Y. Torres, D. Casellas, M. Anglada, L. Llanes, Fracture toughness evaluation of hardmetals: influence of testing procedure, Int. J. Refract. Met. Hard Mater. 19 (2001) 27–34.

[34] ASTM E 1876-01: Standard test method for dynamic Young's Modulus, Shear Modulus, and Poisson's Ratio by impulse excitation of vibration, USA, 2001.

[35] B. Casas, X. Ramis, M. Anglada, J.M. Salla, L. Llanes, Oxidation-induced strength degradation of WC–Co hardmetals, Int. J. Refract. Met. Hard Mater. 19 (2001) 6–12.

[36] X. Shi, H. Yang, G. Shao, X. Duan, S. Wang, Oxidation of ultrafine-cemented carbide prepared from nanocrystalline WC–10Co composite powder, Ceram. Int. 34 (2008) 2043–2049.

[37] J.A. Yeomans, Ductile particle ceramic matrix composites—Scientific curiosities or engineering materials?, J. Eur. Ceram. Soc. 28 (2008) 1543–1550.

[38] W.-L. Wang, J.-Q. Bi, K.-N. Sun, M. Du, N.-N. Long, Y.-J. Bai, Thermal shock resistance behavior of alumina ceramics incorporated with boron nitride nanotubes, J. Am. Ceram. Soc. 94 (2011) 2304–2307.

[39] T.J. Lu, N.A. Fleck, The thermal shock resistance of solids, Acta Mater. 46 (1998) 4755–4768.

[40] G. Gille, B. Szesny, K. Dreyer, H. van den Berg, J. Schmidt, T. Gestrich, G. Leitner, Submicron and ultrafine grained hardmetals for microdrills and metal cutting inserts, Int. J. Refract. Met. Hard Mater. 20 (2002) 3–22.

[41] H. Wang, T. Webb, J.W. Bitler, Study of thermal expansion and thermal conductivity of cemented WC–Co composite, Int. J. Refract. Met. Hard Mater. 49 (2015) 170–177.

[42] B. Wittmann, W.-D. Schubert, B. Lux, WC grain growth and grain growth inhibition in nickel and iron binder hardmetals, Int. J. Refract. Met. Hard Mater. 20 (2002) 51–60.

[43] K. Bonny, P. De Baets, J. Vleugels, S. Huang, B. Lauwers, Dry reciprocating sliding friction and wear response of WC-Ni cemented carbides, Tribol. Lett. 31 (2008) 199–209.

[44] R.M. Genga, G. Akdogan, C. Polese, J.C. Garrett, L.A. Cornish, Abrasion wear, thermal shock and impact resistance of WC-cemented carbides produced by PECS and LPS, Int. J. Refract. Met. Hard Mater. 49 (2015) 133–142.

[45] S. Lay, J.-M. Missiaen, Microstructure and morphology of hardmetals, in: V.K. Sarin, D. Mari, L. Llanes (Eds.), Comprenhensive Hard Materials, Elsevier, UK, 2014: pp. 91–120.

[46] B. Roebuck, E.A. Almond, The influence of composition, phase transformation and varying the relative F.C.C. and H.C.P. phase contents on the properties of dilute Co-W-C Alloys, Mater. Sci. Eng. 66 (1984) 179–194.

[47] J.M. Marshall, M. Giraudel, The role of tungsten in the Co binder: Effects on WC grain size and hcp–fcc Co in the binder phase, Int. J. Refract. Met. Hard Mater. 49 (2015) 57–66.

[48] E.F. Drake, A.D. Krawitz, Fatigue damage in a WC-Nickel cemented carbide composite, Metall. Mater. Trans. A. 12A (1981) 505–513.

[49] C.H. Vasel, A.D. Krawitz, E.F. Drake, E.A. Kenik, Binder deformation in WC-(Co, Ni) cemented carbide composites, Metall. Mater. Trans. A. 16A (1985) 2309–2317.

[50] L. Llanes, B. Casas, E. Idañez, M. Marsal, M. Anglada, Surface Integrity Effects on the Fracture Resistance of Electrical-Discharge-Machined WC-Co Cemented Carbides, J. Am. Ceram. Soc. 87 (2004) 1687–1693.

[51] J. Yang, M. Odén, M.P. Johansson-Jõesaar, L. Llanes, Grinding Effects on Surface Integrity and Mechanical Strength of WC-Co Cemented Carbides, Procedia CIRP. 13 (2014) 257–263.

[52] G.R. Irwin, Fracture, in: Handbook Der Physics, Springer-Verlag, Berlin, 1958.

[53] J.P. Singh, Effect of flaws on the fracture behavior of structural ceramics: A review, Adv. Ceram. Mater. 3 (1988) 18–27.

LIST OF FIGURES

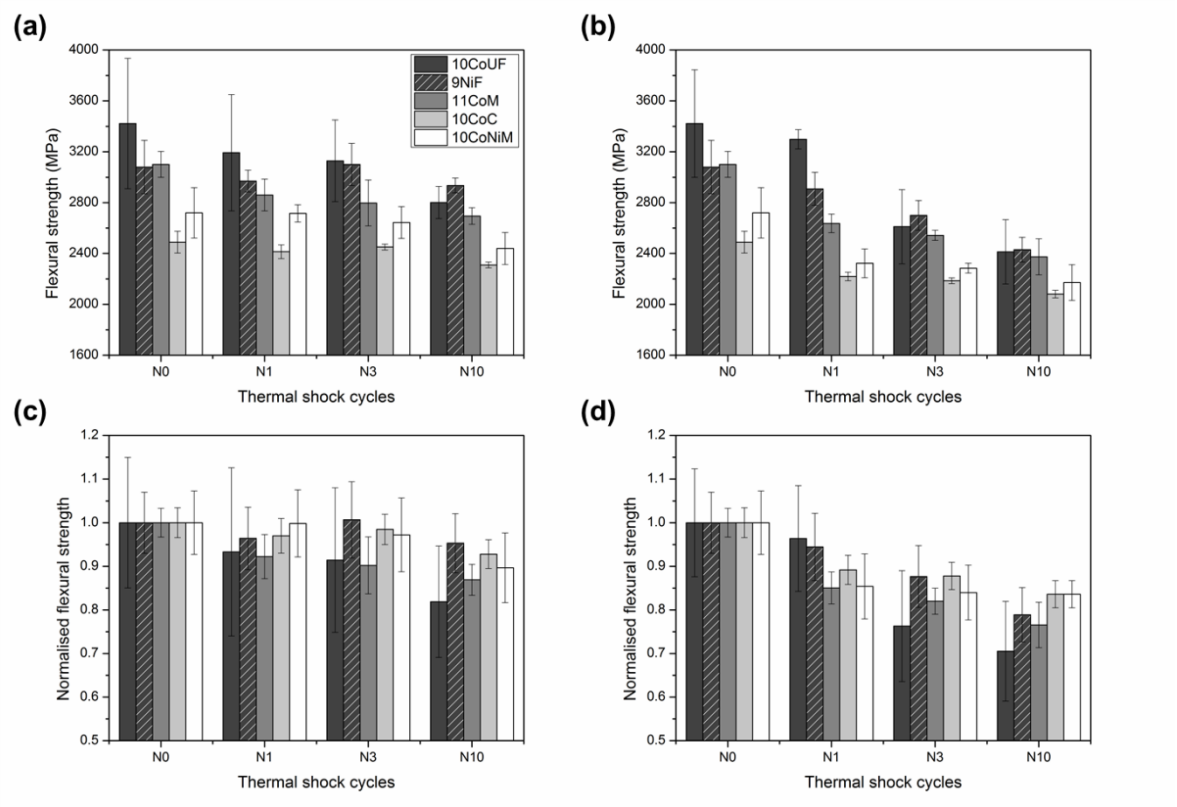

Figure 1. Flexural strength as a function of the number of quenching cycles (N_i) at the two investigated temperature differentials of (a) 400ºC and (b) 550ºC for the investigated hardmetals. The same results are displayed as the normalized flexural strength for the (c) 400ºC and (d) 550ºC investigated temperature differentials, by using the strength of non-quenched specimens as reference baselines.

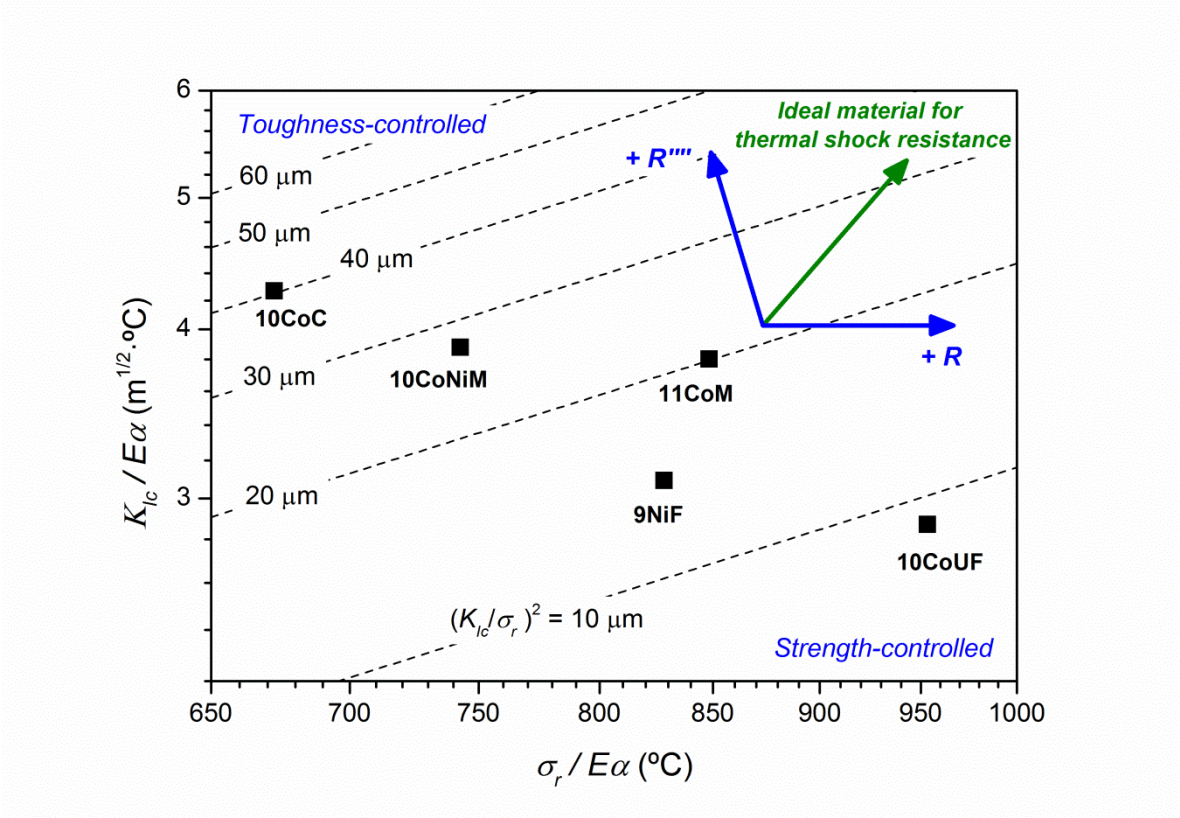

Figure 2. Merit index for strength-controlled failure ($\sigma_r/E\alpha$) against merit index for toughness-controlled failure ($K_{Ic}/E\alpha$). Straight dashed lines represent the evolution of the $(K_{Ic}/\sigma_r)^2$ ratio, directly proportional to the R'''' Hasselman parameter. The ideal material against thermal shock degradation would be the one combining high values for both merit indices.

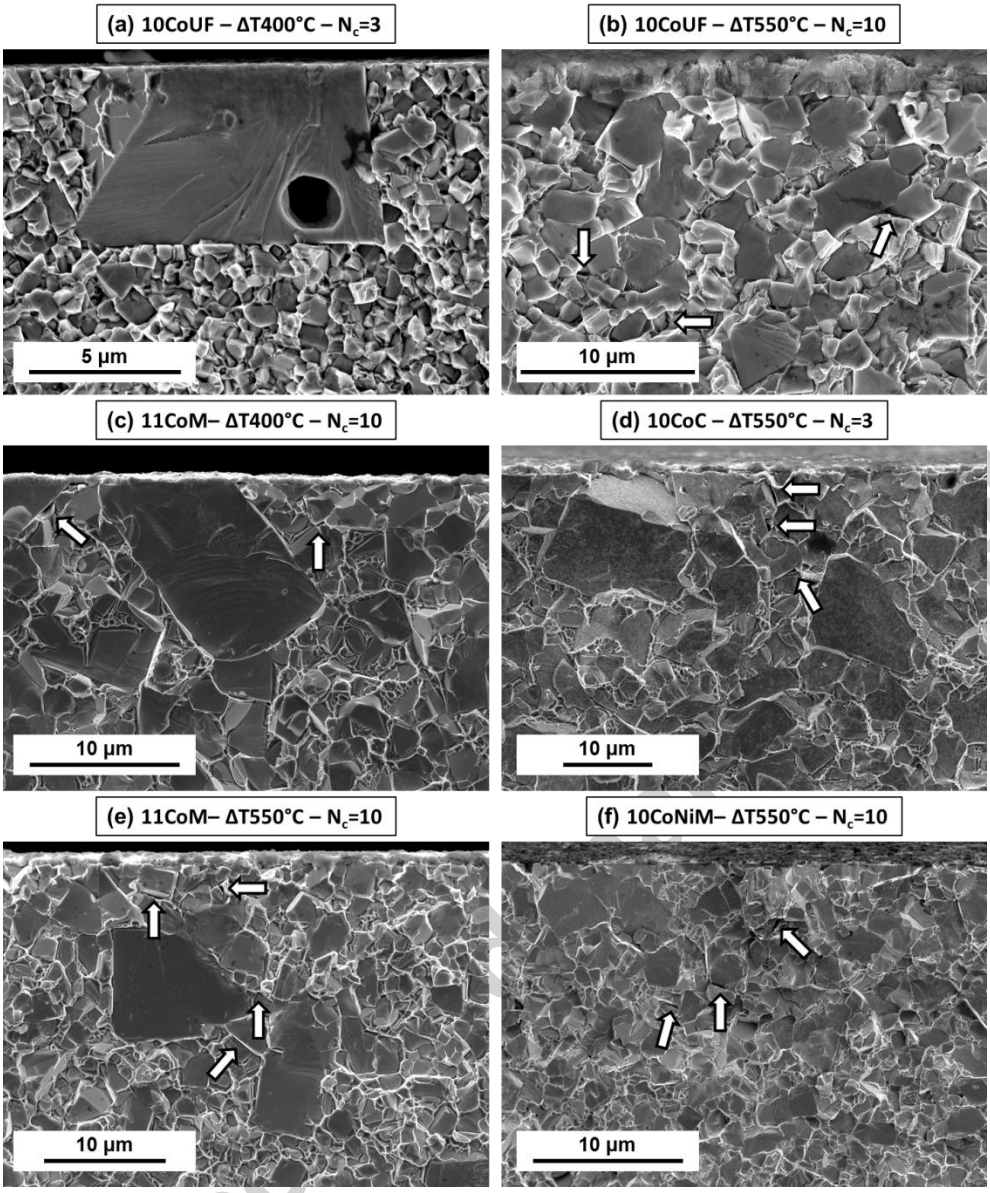

Figure 3. Micrographs corresponding to critical flaws that promoted failure in investigated materials after being subjected to single and/or repetitive thermal shocks. They correspond to two generic types. First, an abnormally coarse WC particle in; (a) and (c). Second, binderless concentration of abnormally coarse WC particles in; (b), (d), (e) and (f). Microcracking in the vicinity of the critical flaws was evidenced and marked with arrows.

a

Table 1. Nomenclature, binder chemical nature and weight content (V^{wt}_{binder}), carbide mean grain size (d_{WC}) and contiguity (C_{WC}), and binder mean free path (λ_{binder}) for the investigated cemented carbides. *Hardmetal grades 10CoUF, 11CoM and 9NiF include a small amount of Cr_3C_2, added as a grain growth inhibitor.

Specimen code	V^{wt}_{binder} ($\%_{wt.}$)	d_{WC} (μm)	C_{WC}	λ_{binder} (μm)
10CoUF*	10.0	0.39 ± 0.19	0.46 ± 0.06	0.16 ± 0.06
11CoM*	11.0	1.12 ± 0.71	0.38 ± 0.07	0.42 ± 0.28
10CoC	10.0	2.33 ± 1.38	0.31 ± 0.11	0.68 ± 0.48
10CoNiM	$7.5\%_{wt.}$Co - $2.5\%_{wt.}$Ni	1.04 ± 0.83	0.41 ± 0.08	0.36 ± 0.29
9NiF*	9.0	0.83 ± 0.49	0.44 ± 0.08	0.29 ± 0.18

Table 2. Hardness (*HV*), Young modulus (*E*), flexural strength (σ_r), fracture toughness (K_{Ic}), Poisson ratio (υ), coefficient of thermal expansion (α) and estimated R and R'''' Hasselman parameters for studied cemented carbides. *Poisson ratio and thermal expansion coefficient were estimated using the rule of mixtures for composite materials.

Specimen code	*HV* (GPa)	*E* (GPa)	σ_r (MPa)	K_{Ic} (MPa)	υ*	α* (ppm/C^o)	*R* (^{o}C)	*R''''* (μm)
10CoUF	15.7 ± 0.6	582 ± 4	3422 ± 512	10.4 ± 0.3	0.24	6.62	677	5.9
11CoM	12.8 ± 0.2	577 ± 3	3101 ± 102	13.9 ± 0.3	0.24	6.75	606	13.2
10CoC	11.4 ± 0.2	595 ± 5	2489 ± 85	15.8 ± 0.3	0.24	6.61	482	26.4
10CoNiM	11.6 ± 0.1	593 ± 3	2720 ± 198	14.2 ± 0.4	0.24	6.57	532	17.9
9NiF	13.2 ± 0.2	612 ± 5	3080 ± 210	11.5 ± 0.2	0.24	6.47	593	9.1

Table 3. Flexural strength for investigated 10CoUF hardmetal measured for water quenched specimens before and after the application of a heat treatment for the relaxation of TRS.

	σ_r (MPa)	
	Water quenched	Water quenched and heat treated
10CoUF – ΔT = 400ºC – 10 cycles	2802 ± 126	2672 ± 248
10CoUF – ΔT = 550ºC – 3 cycles	2611 ± 292	2885 ± 246
10CoUF – ΔT = 550ºC – 10 cycles	2413 ± 253	2442 ± 227

Table 4. Estimated critical flaw sizes according to LEFM equation by considering the defects as semicircular surface cracks.

Specimen code	Non-quenched	ΔT = 400 ºC			ΔT = 550 ºC		
		N_c = 1	N_c = 3	N_c = 10	N_c = 1	N_c = 3	N_c = 10
10CoUF	6	6	7	8	6	10	11
11CoM	12	14	15	16	17	18	21
10CoC	24	26	25	28	30	31	35
10CoNiM	16	16	17	20	22	23	26
9NiF	8	9	8	9	9	11	13